Nat. Hazards Earth Syst. Sci. Discuss., 1, 1619–1649, 2013
www.nat-hazards-earth-syst-sci-discuss.net/1/1619/2013/
doi:10.5194/nhessd-1-1619-2013

Natural Hazards and Earth System Sciences
Discussions
Open Access

Estimation of the effects of climate change on flood-triggered economic losses in Japan

S. Tezuka[1], H. Takiguchi[2], S. Kazama[1], R. Sarukkalige[3], A. Sato[1], and S. Kawagoe[4]

[1]Graduate School of Environmental Studies, Tohoku University, 6-6-20, Aramaki aza aoba, Aoba ku, Sendai, 981-8579, Japan
[2]Department of Civil Engineering, Tohoku University, 6-6-06, Aramaki aza aoba, Aoba ku, Sendai, 981-8579, Japan
[3]Department of Civil Engineering, Curtin University, G.P.O. Box U1987, Perth, WA 6845, Australia
[4]Division of Environmental System Management, Faculty of Symbiotic Systems Science, Fukushima University, 1, Kanayagawa, Fukushima, 980-1296, Japan

Received: 10 April 2013 – Accepted: 19 April 2013 – Published: 24 April 2013

Correspondence to: R. Sarukkalige (p.sarukkalige@curtin.edu.au)

Published by Copernicus Publications on behalf of the European Geosciences Union.

Abstract

This study evaluates the effects of climate change on economic losses due to flood-related damage in Japan. Three selected GCM climate data were downscaled using an analytical method that uses observed precipitation data as the reference resolution. The downscaled climate data were used to estimate extreme rainfall for different return periods. The extreme rainfall estimates were then entered into a two-dimensional (2-D) non-uniform flow model to estimate flood inundation information. A novel technique based on the land use type of the flood area was employed to estimate economic losses due to flood damage. The results of the rainfall analysis shows that at present (in 2000), the Nankai region, the area from Wakayama Prefecture to Kagoshima Prefecture and the mountains of the Japan Alps receive very high extreme rainfall. By 2050, in addition to these areas, the rainfall in the Tokai and Koshinetsu regions will be 1.2 to 1.3 times greater than at present. The flood-related economic loss estimation shows that the relationship between increased extreme rainfall and increased potential economic loss due to flood damage has a nearly linear relationship. The overall variations show that the potential economic loss is greater for the SRES-B1, A2 and A1B scenarios for all return periods. These results clearly show that flood-related economic losses in Japan will increase significantly in the future as a result of climate change.

1 Introduction

In recent years, the effects of climate change on natural disasters have attracted significant attention among researchers and the public. Cyclones, typhoons, floods, landslides and other slope hazards are major natural disasters triggered by the effects of climate change. Growing attention to the threats posed by the effects of climate change on natural disasters has led to increasing contact and interaction between the fields of climate change adaptation and disaster risk reduction (Solecki, et al., 2011). In addition, authorities, decision makers and policy makers have responded

NHESSD
1, 1619–1649, 2013

to the public's needs for vulnerability reduction and resilience improvement to adapt to climate-change-induced disasters (Smit and Wandel, 2006; Saavedra and Budd, 2009). Several studies related to natural disasters and climate change have highlighted the ways in which climate change alters disaster risks and the contributions that disaster risk reduction can make to climate change adaptation (Helmer and Hilhorst, 2006; O'Brien et al., 2006; Mercer, 2010; Hori and Shaw, 2011).

The literature highlights several major studies on the effects of climate change on natural disasters in Japan (Kawagoe et al., 2010; Mouri et al., 2012; Izumi et al., 2012). Flood is one of the major types of natural disasters that occur in Japan (Grossman, 2001; Kazama et al., 2009, Mouri et al., 2011). Therefore, it is very important to evaluate how future climate change may alter the probability of flood disasters. Due to the steep geography and humid climate, Japan is particularly vulnerable to flooding (Kazama et al., 2009). Increases in the frequency and intensity of local heavy storms of torrential rain have been recorded in Japan in recent years (Niigata and Fukushima: 12–13 July 2004; Fukui: 17–18 July 2004; Miyazaki: 4–7 September 2005; Chugoku and Kyushu: 19–26 July 2009; Amami: 18–21 October 2010; Niigata and Fukushima: 27–30 July 2011; Kyushu: 11–14 July 2012). All of these heavy rainfalls created local floods and heavy damage, leading to significant economic losses. Literature shows that Japan has been coping with the issues related to flood control for a long time (Miyata and Abe, 1994; Takahasi and Uitto 2004; Yoshikawa et al., 2004; Kazama et al., 2009). The frequency of floods and the damage caused by flooding has increased since 2004 (Kazama et al., 2009). In 2008, the Japanese government organized a committee of experts to implement in-house flood control policies (MLIT, 2008). However, torrential rains associated with climate change create floods that exceed current design criteria, and current flood control measures are not adequate to address such floods (Mouri et al., 2012). The damage caused by these floods calls attention to the necessity of updated flood control measures that take the potential effects of future climate change into account.

NHESSD
1, 1619–1649, 2013

Global climate models (GCMs) are the basic source of projections of future trends in various climate variables. These models can simulate climate projections at the global or continental scale quite reliably but are not accurate enough at the regional scale (Piani et al., 2010; Jeong et al., 2012). This inaccuracy is because the spatial resolution of GCM grids is too coarse to resolve many important sub-grid scale processes (most notably those pertaining to the hydrological cycle) and because GCM output is often unreliable at the individual grid and sub-grid box scales (IPCC, 2007). The general procedure for assessing the effects of climate change is to first project future climate change with GCM simulations, then downscale climate projections from the global to the regional scale, and then generates predictions using numerical models and climate change simulations (Bae et al., 2011).

Three GCM data sources (MIROC3.2, CGCM2.3.2 and PCM) were used in this study to evaluate the effects of future climate change on flood disasters in Japan. As the spatial resolutions of the selected GCMs are very coarse (280 km × 280 km), an analytical downscaling method was used to downscale the data into a fine resolution of 1 km × 1 km. The downscaled climate change data were used to estimate extreme rainfall data, and these data were used to estimate flood inundation using a 2-D non-uniform flow model. A novel approach was used to estimate the economic loss due to flooding and to predict future damage, which is useful in developing sustainable flood mitigation and adaptation procedures.

2 Methodology and data

The methodology for predicting future economic losses due to flood damage triggered by climate change involves downscaling the collected GCM precipitation data to a fine resolution that is compatible with regional-scale evaluations. We also used a numerical approach to simulate flood inundation and estimate the associated flood depth, inundation period and inundation area for use in estimating flood damage.

NHESSD
1, 1619–1649, 2013

2.1 Regional climate downscaling

Three sets of GCM data were used for the assessment: MIROC3.2 co-developed by the Center for Climate System Research (CCSR), the National Institute for Environmental Studies (NIES) and the Frontier Research Center for Global Change (FRCGC); CGCM2.3.2, developed by the Japanese Meteorological Research Institute; and PCM, developed by the National Centre for Atmospheric Research in Japan (K-1 Model developers, 2004). These models were developed by the Meteorological Research Institute and other domestic research organizations, and they offer the advantage that additional detailed information about the whole of Japan is provided. All of these models have a horizontal resolution of 280 km × 280 km, which creates 18 grid cells covering all of Japan. To evaluate the effects of different climate scenarios on flood damage, we used three SRES scenarios: A1B, A2 and B1.

Mesh Climate Value 2000, produced by the Japan Meteorological Agency (JMA, 2002), was used as the main reference data set for the analytical downscaling process. The resolution of Mesh Climate Value 2000 is 1 km × 1 km. These data are produced using precipitation observation data from AMeDAS (the Automated Meteorological Data Acquisition System). As the mean monthly precipitation data are used for the analysis, mean monthly precipitation data from GCM models are downscaled to fine resolution using the following equation.

$$P_i = \mathrm{Bd}_i \times \mathrm{Gf}_j \quad (1)$$

where P = monthly precipitation after downscaling (mm), Bd = fine resolution factor, Gf = monthly precipitation obtained from GCM model data (mm), and i, j = elements of 1- and 280 km resolution data sets.

The fine resolution factor (Bd) is the main governing factor in developing the downscaled precipitation value for a given location. The fine resolution factor (Bd) is defined as the ratio between the Mesh Climate Value and the present precipitation data of the

NHESSD
1, 1619–1649, 2013

GCM model considered at a resolution of 1 km × 1 km, as shown below.

$$\mathrm{Bd}_i = \frac{\text{Mesh climate Model precipitation value}_i\ (1\,\text{km} \times 1\,\text{km resolution})}{\text{GCM model present precipitation value}_i\ (1\,\text{km} \times 1\,\text{km resolution})} \quad (2)$$

To minimize the resolution of the present climate data of the given GCM model data to 1 km × 1 km resolution, we used the inverse distance weighing method. Bd represents regional characteristics of rainfall that depend on the geographic features of the area. This method permits the generation of smooth- and fine-resolution spatial distributions of precipitation over Japan. Figure 1 shows the distribution of the fine-resolution factor (Bd) over Japan for the MIROC3.2 model under the A1B and A2 SRESS scenarios.

2.2 Calculation of extreme rainfall and return period

Extreme rainfall for several return periods (5 yr, 10 yr, 30 yr, 50 yr and 100 yr) was estimated by analyzing the maximum recorded 24 h precipitation data for a period of 20 yr (1980–2000), obtained from 1024 AMeDAS (Automated Meteorological Data Acquisition System) meteorological data observation stations. To develop the extreme rainfall distributions, 24 h maximum rainfall values were obtained by frequency analysis using AMeDAS observation data. In the frequency analysis of extreme rainfall for various return periods, the generalized extreme value distribution function (GEV) was used as the probability distribution. The probability weight moment method (PWM) was used as the universal prediction method. The GEV distribution function, which is the extreme rainfall event distribution, is the asymptotic distribution of the maximum and minimum values in the universe. Therefore, it is an effective probability distribution for estimating the expected maximum value of rainfall.

NHESSD
1, 1619–1649, 2013

In the first step, the PWM method is used to obtain the probability weight moment as explained by Kawagoe et al., (2010):

$$\begin{cases} \beta_0 = \frac{1}{N}\sum_{j=1}^{N} x_{(j)} \\ \beta_1 = \frac{1}{N(N-1)}\sum_{j=1}^{N} (j-1)\, x_{(j)} \\ \beta_2 = \frac{1}{N(N-1)(N-2)}\sum_{j=1}^{N} (j-1)(j-2)\, x_{(j)} \end{cases} \quad (3)$$

where N is the number of sample data, j is the rank, and $x_{(j)}$ is the set of values of smaller rank in the sample data for which the maximum daily rainfall data in the AMeDAS data set from 1980 to 2000 are used. The product moment λ is obtained as a function of the probability weight moment β.

The population parameter k is obtained as a function of the probability weight moment β and the product moment λ.

$$k = 7.8590\left(\frac{2\lambda_2}{\lambda_3 + 3\lambda_2} - \frac{\ln(2)}{\ln(3)}\right) \quad (4)$$

The scale parameter a and location parameter c are obtained using the population parameter k and the product moment λ.

$$\begin{cases} a = \frac{k\lambda_2}{(1-2^{-k})\Gamma(1+k)} \\ c = \lambda_1 - \left(\frac{a}{k}\right)[1 - \Gamma(1+k)] \end{cases} \quad (5)$$

The CDF (cumulative distribution function) $F(x)$ of the GEV distribution is obtained from the following equation as a function of the population parameter k, the scale parameter a and the location parameter c.

$$F(x) = \exp -\left[1 - \left(\frac{a}{k}\right)(x-c)\right]^{1/k} \quad (6)$$

NHESSD
1, 1619–1649, 2013

The extreme heavy rainfall corresponding to a return period of T years is obtained from the following equation.

$$\begin{cases} x_T = c + \left(\frac{a}{k}\right)\left\{1 - [-\ln(p)]^k\right\} \\ p = 1 - (1/T) \end{cases} \quad (7)$$

where T is the return period and p is the non-exceed probability.

To evaluate the spatial distribution of maximum rainfall for each return period, linear regression analysis was used to develop a relationship between the extreme rainfall data and the annual mean precipitation data. The annual mean precipitation data were obtained from Mesh Climate Value 2000 (JMA, 2002). The inverse distance weighted method and the Thiessen method were used to interpolate precipitation values for use in the regression analysis.

Because this study was mainly concerned with rainfall as the precipitation component, in the winter season, only precipitation in the form of rainfall (warm day precipitation) was taken into account. The widely used 20 °C threshold was used to determine the rainfall and snowfall (Singh and Bengtsson, 2005; Kazama et al., 2008, Kawagoe et al., 2009). Only rainfall events were considered in conducting the regression analysis. Snowfall events were omitted from regression analysis. This rainfall-snowfall separation method allowed to estimate different regression coefficients for different seasons (Ushiyama and Takara, 2003). Assuming that the spring rainfall is from March to May, the summer rainfall is from June to August, the autumn rainfall is from September to November, and the winter rainfall is on warm days (days with average temperatures greater than 20 °C) from December to February, regression relations between maximum monthly rainfall and 24 h extreme rainfall were developed for each season (Kawagoe, 2010). The mountainous areas on the western side of Japan (the Japan Sea side) receive most of their precipitation during the winter. Other areas of Japan receive most of their precipitation during the summer and autumn (June to November). Only the southern islands of Japan receive most of their precipitation in the spring. Therefore, summer and spring rainfalls are grouped together, and separate regression analyses

NHESSD
1, 1619–1649, 2013

were carried out for areas with their maximum rainfall in autumn, winter, and spring + summer (Kawagoe, 2010).

The relationships between maximum monthly rainfall in each season and the 24 h extreme rainfall for a 30 yr return period are shown in Fig. 2. As the regression relationship between maximum monthly rainfall and extreme daily rainfall changes seasonally, regression analysis was carried out considering each seasonal data set separately for five selected return periods (5 yr, 10 yr, 30 yr, 50 yr and 100 yr). A linear regression equation can be developed between the daily maximum rainfall and monthly maximum rainfall as follows:

$$R_{dm} = a\,R_{mm} + b \tag{8}$$

where R_{dm} is the daily maximum rainfall, R_{mm} is the monthly maximum rainfall and a and b are regression coefficients.

Table 1 summarizes the correlation between maximum monthly rainfall and daily extreme rainfall for 10 yr, 30 yr and 100 yr return periods. It clearly shows the difference of the correlation in different seasons. The estimated extreme rainfall values were then entered as the main input into a two-dimensional (2-D) non-uniform flow model to estimate flood inundation information.

2.3 Flood inundation model

The inundation model used in this study is a two-dimensional non-uniform flood flow model (Kazama et al., 2009). The model uses Manning's roughness method to take land use type into account. The Manning's roughness values were estimated by calibration the model against many Japanese basins (Kazama et al., 2009). Geographical Survey Institute (GSI) of Japan provided the land use data for the study areas. Extreme rainfall data from continuous periods of 24 h are obtained according to the methodology described in Sect. 2.2. Estimated extreme rainfall data were used as the input data to the inundation model.

NHESSD
1, 1619–1649, 2013

According to the steep topography of Japan, a flood wave caused by extreme rainfall in most rivers can reach the river mouth within a short period (less than 24 h), except in a few cases (Kazama et al., 2009). Following data input, the inundation simulation was carried out for 1 week to determine the maximum water depth, inundation period, and inundation distribution needed to calculate flood damage costs.

The 2-D non-uniform flow models used in the inundation calculation are shown in the following equations (Chow et al., 1988; Kazama et al., 2007, 2009). This model consists of the continuity equation and 2-D momentum equation;

Continuity equation:

$$\gamma\frac{\partial D}{\partial t}+\frac{\partial \gamma M}{\partial x}+\frac{\partial \gamma N}{\partial y}=0 \tag{9}$$

where $M = uD$ is the discharge flux in the x direction ($m^2\,s^{-1}$) and $N = vD$ is the discharge flux in the y direction ($m^2\,s^{-1}$). v and u are the velocity ($m\,s^{-1}$) in the x and y directions.

Momentum in the x direction:

$$\lambda\frac{\partial M}{\partial t}+\frac{\partial}{\partial x}\left(\lambda\frac{M^2}{D}\right)+\frac{\partial}{\partial y}\left(\lambda\frac{MN}{D}\right)+\gamma gD\frac{\partial (D+h)}{\partial x}+\gamma gn^2\frac{M\sqrt{M^2+N^2}}{D^{7/3}}+\frac{1}{2}\frac{(1-\gamma)}{B}C_D\frac{M\sqrt{M^2+N^2}}{D}=0 \tag{10}$$

Momentum in the y direction:

$$\lambda\frac{\partial N}{\partial t}+\frac{\partial}{\partial x}\left(\lambda\frac{MN}{D}\right)+\frac{\partial}{\partial y}\left(\lambda\frac{N^2}{D}\right)+\gamma gD\frac{\partial (D+h)}{\partial y}+\gamma gn^2\frac{N\sqrt{M^2+N^2}}{D^{7/3}}+\frac{1}{2}\frac{(1-\gamma)}{B}C_D\frac{N\sqrt{M^2+N^2}}{D}=0 \tag{11}$$

NHESSD
1, 1619–1649, 2013

The relationship between λ and γ is expressed as follows:

$$\lambda = \gamma + (1 - \gamma) C_M \tag{12}$$

where g is gravitational acceleration ($m\,s^{-2}$), h is the elevation (m), n is Manning's coefficient ($s\,m^{-1/3}$), D is the water depth (m), $(1 - \gamma)$ is the house occupancy ratio, B is the house size (m), C_M is the additive mass coefficient (= 0.2), and C_D is the house drag coefficient (= 1.0). It was assumed that B and γ can be taken as constants (14.941 and 0.411 respectively) for residential land use, according to the flood control economy investigation manual (MLIT, 2005). Even though the nonlinear terms are included in the original flow equations, this estimation ignored them to avoid complex calculations. The time interval and ground resolution of the model were selected as 1 s and 1 km respectively. Values for Manning's coefficient for inundation flow are given in hydraulics formulas as a function of land use (JSCE, 1999). Finite difference method expressing a forward difference scheme in time and a central difference scheme in space are used to solve these equations (Kazama et al., 2009). Kazama et al. (2002) tested this 2-D non-uniform flow model in the eastern part of Sendai City in Japan and confirmed the accuracy of the model.

2.4 Estimation of the economic loss due to flood damage

The methods described by flood control economy investigation manual (MLIT, 2005) is used to calculate the cost of flood damage for each type of land use. Land use grid data (KS-META-L03-09 M) (National Land Information Office, 2007) were used as the main land use data. The land use types are categorized to; (1) paddy fields, (2) other agricultural lands, (3) residential areas, (4) golf courses, and (5) traffic zones. Damage was not considered for other land use types, such as forests, bare lands, rivers and lakes, and beaches. The calculation method used for each type of land use is explained below.

NHESSD
1, 1619–1649, 2013

2.4.1 Economic loss in agricultural lands

Agricultural damage in paddy fields and other agricultural lands was calculated by multiplying agricultural assets by the damage rate corresponding to the inundation depth and inundation period. The agricultural assets were calculated as the product of cultivated surface area and the price of agricultural production per unit area (Kazama et al., 2009).

Paddy field damage was calculated using the following formula:

$$\begin{aligned}\text{damage(USD)} = 489(\text{t km}^{-2}) &\times 2480\ (\text{USD t}^{-1}) \times \text{inundation area}\,(\text{km}^2) \\ &\times \text{damage rate by inundation depth}\end{aligned} \tag{13}$$

where 489 t km^{-2} is the national median of the average harvest volume per unit area of paddy fields in Japan and 2480 USD t^{-1} is the unit price of rice in Japan (Kazama et al., 2009).

To determine the damage in other agricultural lands in Japan, tomatoes were selected to represent Japanese agricultural production as they are widely grown throughout the country. In fact, the average agricultural production is approximately 2360 USD t^{-1} (MAFF, 2002). Tomato production, with an average annual yield of 2300 USD t^{-1}, approximates this value closely. Therefore average agricultural production is well represented by tomato.

Damage to other agricultural lands was determined using the following formula:

$$\begin{aligned}\text{damage (USD)} = 5770\ (\text{t km}^{-2}) &\times 2300\ (\text{USD t}^{-1}) \times \text{inundation area}\,(\text{km}^2) \\ &\times \text{damage rate by inundation depth}\end{aligned} \tag{14}$$

where 5770 t km^{-2} is the national median of the average volume of tomatoes harvested per unit of land area in Japan and 2300 USD t^{-1} is the unit price of tomatoes in Japan.

Even though the cost of agricultural damage depends on the stage of crop growth, this estimation did not consider the timing of flooding, and it was assumed that the worst case of damage occurred at the harvesting season of the crops.

NHESSD
1, 1619–1649, 2013

2.4.2 Economic loss in residential areas

Residential lands with strong economic activities such as houses and office buildings and commercial establishments, get the highest damage during floods. Residential land use can be divided into two subcategories, residential buildings and office buildings. Based on national data on land use, reutilization changes, and economic and policy changes (site mesh KS-METAA02- 60 M) (National Land Information Office, 2007), damages to residential buildings can be estimated as;

$$\text{residential building damage} = \text{building damage} + \text{household furniture damage} \quad (15)$$

and damages to office buildings can be estimated as;

$$\text{office building damage} = \text{building damage} + \text{redemption and inventory assets} \quad (16)$$

Damage to residential houses was calculated by multiplying the average house assets in each prefecture by the damage rate as a function of the water. House assets data were obtained from the MLIT (2005), and the damage rate was obtained directly from empirical data from the MLIT (2005):

$$\begin{aligned}\text{house damage (USD)} &= \text{house assets (USD m}^{-2}) \times \text{inundation area (m}^2) \\ &\times \text{damage rate by inundation depth}\end{aligned} \quad (17)$$

Economic damage to household furniture was calculated by multiplying household furniture assets by the damage rate for the flood depth. Household furniture assets were calculated by multiplying the number of households by the average unit price per household:

$$\begin{aligned}\text{house furniture damage(USD)} &= 129\,720(\text{USD household}^{-1}) \\ &\times \text{inundated household (household)} \\ &\times \text{damagerate by inundation depth}\end{aligned} \quad (18)$$

NHESSD
1, 1619–1649, 2013

where 129 720 USD m^{-2} is the national median value of a household in Japan in 2004.

Economic damage to office building was calculated in the same way. Office damage was calculated by multiplying office depreciable assets and inventory assets by the damage rate for the flood depth evaluated by the inundation model. Office depreciable assets and inventory assets were calculated by multiplying the number of employees by the unit price per employee:

$$\begin{aligned}\text{depreciable asset damage(USD)} = {} & 56\,210(\text{USD employee}^{-1}) \\ & \times \text{inundation influence working force(employee)} \\ & \times \text{damage rate by inundation depth}\end{aligned} \quad (19)$$

$$\begin{aligned}\text{inventory asset damage(USD)} = {} & 49\,150(\text{USD employee}^{-1}) \\ & \times \text{inundation influence working force(employee)} \\ & \times \text{damage rate by inundation depth}\end{aligned} \quad (20)$$

where 56 210 USD employee^{-1} is the average value of depreciable assets per employee in Japan and 49 150 USD employee^{-1} is the average value of inventory assets per employee in Japan (except in agriculture, forestry, and fisheries).

2.4.3 Economic loss in golf courses

Depreciable assets and inventory assets were used to estimate flood damage in golf course areas as follows;

$$\text{golf course damage} = \text{depreciable assets} + \text{inventory assets(service industry)} \quad (21)$$

NHESSD
1, 1619–1649, 2013

where;

$$\text{depreciable asset damage(USD)} = 42\,360(\text{USD employee}^{-1}) \times \text{inundation influence working force(employee)} \times \text{damagerate by inundation depth} \quad (22)$$

$$\text{inventory asset damage(USD)} = 3200(\text{USD employee}^{-1}) \times \text{inundation influence working force(employee)} \times \text{damagerate by inundation depth} \quad (23)$$

where 42 360 USD employee^{-1} is the average value of depreciable assets per employee and 3200 USD employee^{-1} is the average value of inventory assets per employee in the service sector in Japan in 2005 (MLIT, 2005).

2.4.4 Economic loss in traffic zones

As it is hard to estimate the economic damage in traffic zones directly, damage in traffic zone was calculated as a function of general asset damage.

$$\text{traffic zone damage} = \text{general asset damage} \times 1.694 \quad (24)$$

General asset damage means the accumulation of house damage, furniture damage and office depreciable assets and inventory asset damage. MLIT (2005) defines 1.694 as the ratio between the cost of damage to public facilities and the cost of damage to general assets.

Flood damage to other land types (e.g., forests, bare land, rivers and lakes, beaches) was negligible compare to above land uses. Therefore other land uses were not considered in the economic assessment. Also the recovery cost for flood damages were not considered for all land use types. Damage should actually be weighted based on local data such as real estate values and the type of industry. This study assumed uniform conditions throughout Japan, based on the MLIT (2005) manual, which does not take into account frequent price changes.

NHESSD
1, 1619–1649, 2013

3 Results and discussions

As mentioned in the description of the methodology, precipitation data for the three selected GCM models (MIROC3.2, CGCM2.3.2 and PCM) were downscaled to a resolution of 1 km × 1 km. Spatial averages of the downscaled precipitation data show that different GCMs predict different increases in future annual average precipitation in Japan. Figure 3 shows the rates of precipitation increase predicted by the three GCMs considered (MIROC3.2, CGCM2.3.2 and PCM) for A1B SRESS scenario. Although the three models predict different increases in every decade, an overall increase in precipitation is predicted by all three. Compared to the annual average precipitation of the base year (year 2000), the annual average precipitation in 2100 is predicted to be 1.08 % to 1.12 % higher. Although Fig. 3 shows the spatially averaged precipitation throughout Japan, it is assumed that there will be slight variations due to increases in the frequency and amount of local heavy rainfall.

The data for the three selected GCM models were used to estimate the 24 h extreme rainfall for 5 yr, 10 yr, 30 yr, 50 yr and 100 yr return periods using probabilistic analysis. Again, different GCMs yield different spatial distributions of extreme rainfall over Japan. Figure 4 shows the distribution of the daily extreme rainfall of the present climate (in 2000) and the daily extreme rainfall in 2050 according to the MIROC GCM model for the SRESS A1B, A2 and B1 scenarios for a 50 yr return period.

At the present time (in 2000), the Nankai region, the area from Wakayama Prefecture to Kagoshima Prefecture and the mountains of the Japan Alps are all high-precipitation areas, with than 300 mm of daily extreme rainfall. By 2050, in addition to these areas, the rainfall in the Tokai and Koshinetsu regions will be 1.2 to 1.3 times greater than at present because of climate change. The overall variation shows that, except in part of the Seto coastal region and the northeastern part of Hokkaido, there are many regions where daily extreme rainfall will be greater than 225 mm. Overall, an increase in extreme rainfall is predicted. In addition, the percentage of Japan's area that receives more than 300 mm of daily extreme rainfall will increase. Comparing three SRESS

NHESSD
1, 1619–1649, 2013

scenarios, in 2050, extreme rainfall is predicted to be highest for scenarios SRES- B1, A2 and A1B, in that order. Therefore, it can be concluded that by 2050, the highest risk of flooding in this economic development-oriented society will be associated with the SRES – A1B scenario.

The 24 h maximum rainfall for each return period is entered into the two-dimensional non-uniform flow model. The flood depth and flood inundation period for every 1 km × 1 km grid are estimated for different GCMs and different SRES scenarios. These variables are then used as inputs to flood damage estimation equations, based on the primary land use of the grid cell. Total economic loss due to flood damage in Japan is estimated by considering the economic loss in each grid cell. The total economic loss was estimated for the three selected GCMs (MIROC3.2, CGCM2.3.2 and PCM) under three SRES scenarios (A1B, A2 and B1) for five different return periods (5, 10, 30, 50 and 100 yr). Figure 5 depicts the relationship between the variation in total economic loss due to flood damage in Japan and extreme rainfall for MIROC GCM data under the A1B, A2 and B1 SRESS scenarios. The A2 scenario is predicted to produce the greatest economic losses for all return periods. With 500 mm of extreme rainfall predicted for a 100 yr return period, the SRESS A2 scenario yields predictions of more than 1200 billion USD in economic losses due to flooding in Japan.

The relationship between extreme rainfall and economic loss provides a platform for decision makers to predict the potential economic loss once precipitation is observed. Figure 6 shows the relationship between increased extreme rainfall and potential economic loss due to flood damage for the current climate and in 2050 considering MIROC GCM data under the A1B, A2 and B1 SRES scenarios for return periods of 5 yr, 10 yr, 30 yr, 50 yr and 100 yr. This relationship was developed assuming that a 5 yr return period's extreme rainfall and a 5 yr return period's economic loss are 1. The rate of growth of extreme rainfall is on the abscissa, and the rate of growth of potential economic loss is on the ordinate. The 10 yr, 30 yr, 50 yr and 100 yr return period extreme rainfall and related total economic losses are plotted against each other. This graph clearly indicates that the relationship between increased extreme rainfall and increased potential

NHESSD
1, 1619–1649, 2013

economic loss due to flood damage is nearly linear. The overall variation shows that the potential economic loss is greater for the SRES- B1, A2 and A1B scenarios, in that order for all return periods. Under the A1B scenario, in 2050, the 100 yr return period flood damage will be approximately 3.5 times greater than the 5 yr return period flood damage. The 5 yr (base year) return period potential damage is approximately 400 billion US$. In the future, extreme rainfall for shorter return periods will be equivalent to the flood damage associated with longer return periods at present. For example, the 50 yr return period flood damage for the current climate and the 30 yr return period flood damage for the future climate are approximately 900 billion US$. Thus, flood protection schemes that can protect against a flood of a 50 yr return period now will only be able to protect against a 30 yr return period flood in the future because of climate change.

In addition, the relationships between extreme rainfall and potential economic loss due to flood damage under the current climate and in 2050 as predicted by the three GCM models (MIROC3.2, CGCM2.3.2 and PCM) for the A1B SRES scenario for return periods of 5 yr, 10 yr, 30 yr, 50 yr and 100 yr are all linear relationships (Fig. 7). The MIROC3.2 results are higher than those predicted using the CGCM2.3.2 and PCM models for all return periods, whereas the PCM and CGCM2.3.2 predictions of extreme rainfall in 2050 for each return period are very similar to those of the current climate for each return period.

These relationships and the resulting estimates of flood damage as a function of extreme rainfall with multiple return periods may be useful to public, economists, and policy and decision makers in planning and designing the flood control measures that will be required in Japan in the future. Overall, the results indicate that Japan needs an increase in capital investment to implement flood control and mitigation measures that will be required in the future.

NHESSD
1, 1619–1649, 2013

4 Conclusions

Flooding is among the major types of natural disasters that occur in Japan. Future climate change may alter the frequency and intensity of floods in Japan. Prediction of the effects of climate change on economic losses due to flood-related damage in Japan was conducted using climate data from three GCMs (MIROC3.2, CGCM2.3.2 and PCM). The GCM climate data were downscaled using an analytical method that employs observed precipitation data as the reference resolution. The downscaled climate data were used to estimate extreme rainfall values for different return periods. The extreme rainfall estimates served as input to a 2-D non-uniform flow model used to estimate flood inundation information. A novel technique was applied to estimate the economic loss due to flood damage.

The results of the rainfall data analysis show the following:

1. In the present climate (in 2000), the Nankai region, the area from Wakayama Prefecture to Kagoshima Prefecture and the mountains of the Japan Alps are high-rainfall areas with more than 300 mm of daily extreme rainfall.

2. By 2050, the Pacific Ocean side of the Kyushu, Shikoku and Kinki regions will have very high daily extreme rainfall.

3. The rainfall in the Tokai and Koshinetsu regions will increase by a factor of 1.2 to 1.3 by 2050 because of climate change.

4. Except for part of the Seto coastal regions and the north-eastern part of Hokkaido, there are many regions in Japan where daily extreme rainfall will be greater than 225 mm.

Economic loss estimation was conducted using the results from the flood inundation model and information on the land use type of each area. The estimation shows that above 500 mm of extreme rainfall for a 100 yr return period, the SRESS A2 scenario will produce more than 1200 billion USD in economic losses due to flooding in Japan.

NHESSD
1, 1619–1649, 2013

Predictions of the effects of climate change show that the economic losses due to flood damage under extreme rainfall for a 50 yr return period under present climate conditions will be similar to those for a 30 yr return period in 2050. The results also show that a nearly linear relationship exists between the increase in extreme rainfall and the increase in potential economic loss due to flood damage. The overall variations show that the potential economic losses will be greatest under the SRES-B1, A2 and A1B scenarios, in that order, for all return periods. These results clearly show that flood-related economic losses in Japan will increase significantly in the future due to climate change. Therefore, necessary mitigation plans and adaptations are highly recommended. The estimates of flood damage produced in this study will be useful to public, economists, and policy and decision makers in planning and designing flood control measures.

Acknowledgements. The authors would like to acknowledge the support of the Global Environment Research Fund (S-4) of the Ministry of Environment of Japan.

References

Bae, D., Jung, W., and Lettenmaier, D. P.: Hydrologic uncertainties in climate change from IPCC AR4 GCM simulations of the Chungju Basin, Korea, J. Hydrol., 401, 90–105, 2011.

Chow, V. T., Maidment, D. R., and Mays, L. W.: Applied Hydrology, McGraw-Hill, New York, 1988.

Grossman, M. J.: Large floods and climatic change during the Holocene on the Ara River, Central Japan, Geomorphology, 39, 21–37, 2001.

Helmer, M. and Hilhorst, D.: Natural disasters and climate change, Disasters, 30, 1–4, doi:10.1111/j.1467-9523.2006.00302.x, 2006.

Hori, T. and Shaw, R.: Incorporation of potential climate change impacts into local disaster risk management in Costa Rica, Risk, Hazards & Crisis in Public Policy 2, 1–30, doi:10.2202/1944-4079.1094, 2011.

Iizumi, T., Takayabu, I., Dairaku, K., Kusaka, H., Nishimori, M., Sakurai, G., Ishizaki, N., Adachi, S. A., and Semenov, M. A.: Future change of daily precipitation indices in Japan:

NHESSD

1, 1619–1649, 2013

a stochastic weather generator-based bootstrap approach to provide probabilistic climate information, J. Geophys. Res., 117, D11114, doi:10.1029/2011JD017197, 2012.

IPCC: Climate Change 2007: The Physical Science Basis. Contribution of Working Group I to the Fourth Assessment Report of the Intergovernmental Panel on Climate Change, edited by: Solomon, S., Qin, D., Manning, M., Chen, Z., Marquis, M., Averyt, K. B., Tignor, M., and Miller, H. L., Cambridge University Press, Cambridge, UK, New York, USA, 996 pp., 2007.

Jeong, D. I., St-Hilaire, A., Ouarda, T. B. M. J., and Gachon, P.: A multi-site statistical downscaling model for daily precipitation using global scale GCM precipitation outputs, Int. J. Climatol., doi:10.1002/joc.3598, in press, 2012.

JMA, Japan Meteorological Agency: Mesh Climatic Data 2000 (CD-ROM), Japan Meteorological Business Support Center, available at: http://www.jmbsc.or.jp/hp/offline/cdoff1.html (last access: 4 February 2013), 2002.

Japan Society of Civil Engineers (JSCE): Hydraulics formulae, Maruzen, 1999 (in Japanese).

K-1 model developers: K-1 Technical Report No. 1, K-1 Coupled GCM (MIROC) Description, edited by: Hasumi, H. and Emori, S., Center for Climate System Research (CCSR), University of Tokyo; National Institute for Environmental Studies (NIES), Frontier Research Center for Global Change (FRCGC), 2004.

Kawagoe, S., Kazama, S., and Sarukkalige, P. R.: Assessment of snowmelt triggered landslide hazard and risk in Japan, Cold Reg. Sci. Technol., 58, 120–129, 2009.

Kawagoe, S., Kazama, S., and Sarukkalige, P. R.: Probabilistic modelling of rainfall induced landslide hazard assessment, Hydrol. Earth Syst. Sci., 14, 1047–1061, doi:10.5194/hess-14-1047-2010, 2010.

Kazama, S., Nagao, M., Muto, Y., and Tada, T.: Flood hydraulics analysis and prediction that considers land use. A river council joint research report, 2002 (in Japanese).

Kazama, S., Hagiwara, T., Sarukkalige, P. R., and Sawamoto, M.: Evaluation of groundwater resources in wide inundation areas of the Mekong River basin, J. Hydrol., 340, 233–243, 2007.

Kazama, S., Izumi, H., Sarukkalige, P. R., Nasu, T., and Sawamoto, M.: Estimating snow distribution over a large area and its application for water resources, Hydrol. Process., 22, 2315–2324, 2008.

Kazama, S., Sato, A., and Kawagoe, S.: Evaluating the cost of flood damage based on changes in extreme rainfall in Japan, Sustain. Sci., 4, 61–69, 2009.

NHESSD

1, 1619–1649, 2013

Khailani, D. K. and Perera, R.: Mainstreaming disaster resilience attributes in local development plans for the adaptation to climate change induced flooding: a study based on the local plan of Shah Alam City, Malaysia, Land Use Policy, 30, 615–627, 2013.
Mercer, J.: Disaster risk reduction or climate change adaptation: are we reinventing the wheel?, J. Int. Dev., 22, 247–264, doi:10.1002/jid.1677, 2010.
MAFF, Ministry of Agriculture, Forestry and Fisheries: Crops statistics, 2002 (in Japanese).
MLIT, Ministry of Land, Infrastructure, Transport and Tourism: Flood damage statistics of 2004, River Bureau, 2004 (in Japanese).
MLIT, Ministry of Land, Infrastructure, Transport and Tourism: The flood control economy investigation manual, River Bureau, 2005 (in Japanese).
MLIT, Ministry of Land, Infrastructure, Transport and Tourism: Interim report of adaptation of water related disasters for global warming, 2008 (in Japanese).
Miyata, Y. and Abe, H.: Measuring the effects of a flood control project: hedonic land price approach, J. Environ. Manage., 42, 389–401, 1994.
Mouri, G., Kanae, S., and Oki, T.: Long-term changes in flood event patterns due to changes in hydrological distribution parameters in a rural–urban catchment, Shikoku, Japan, Atmos. Res., 101, 164–177, 2011.
Mouri, G., Shinoda, S., Golosov, V., Shiiba, M., Hori, T., Kanae, S., Takizawa, S., and Oki, T.: Ecological and hydrological responses to climate change in an urban-forested catchment, Nagara River basin, Japan, Urban Climate, 1, 40–54, 2012.
National Land Information Office, Ministry of Land, Infrastructure, Transport and Tourism- MLIT, available at: http://nlftp.mlit.go.jp/ksj/ (last access: 18 February 2013), 2007.
O'Brien, G., O'Keefe, P., Rose, J., and Wisner, B.: Climate change and disaster management, Disasters, 30, 64–80, doi:10.1111/j.1467-9523.2006.00307.x, 2006.
Piani, C., Weedon, G. P., Best, M., Gomes, S. M., Viterbo, P., Hagemann, S., and Haerter, J. O.: Statistical bias correction of global simulated daily precipitation and temperature for the application of hydrological models, J. Hydrol., 395, 199–215, 2010.
Saavedra, C. and Budd, W. W.: Climate change and environmental planning: working to build community resilience and adaptive capacity in Washington State, USA, Habitat Int., 33, 246–252, 2009.
Singh, P. and Bengtsson, L.: Impact of warmer climate on melt and evaporation for the rainfed, snowfed and glacierfed basins in the Himalayan region, J. Hydrol., 300, 140–154, 2005.

NHESSD
1, 1619–1649, 2013

Smit, B. and Wandel, J.: Adaptation, adaptive capacity and vulnerability, Global Environ. Chang., 16, 282–292, 2006.
Solecki, W., Leichenko, R., and O'Brien, K.: Climate change adaptation strategies and disaster risk reduction in cities: connections, contentions, and synergies, Current Opinion in Environmental Sustainability, 3, 135–141, 2011.
Takahasi, Y. and Uitto, J. I.: Evolution of river management in Japan: from focus on economic benefits to a comprehensive view, Global Environ. Chang., 14, 83–91, 2004.
Ushiyama, M. and Takara, K.: Relationship between warm season and highest hourly and daily precipitation based AMeDAS data, Journal of Japan society of hydrology and water resources, 13, 368–374, 2003.
Wisner, B.: Untapped potential of the world's religious communities for disaster reduction in an age of accelerated climate change: an epilogue and prologue, Religion, 40, 128–131, 2010.
Yoshikawa, N., Nagao, N., and Misawa, S.: Evaluation of the flood mitigation effect of a Paddy Field Dam project, Agr. Water Manage., 97, 259–270, 2010.

NHESSD
1, 1619–1649, 2013

Table 1. Correlation between maximum monthly rainfall and daily extreme rainfall.

Return period (yr)	Season	Correlation factor	Regression equation Coefficient (*a*)	Regression equation Intercept (*b*)
10	Spring, Summer	0.66	0.37	53.39
	Autumn	0.77	0.60	26.68
	Winter	0.71	0.36	39.91
30	Spring, Summer	0.69	0.53	88.10
	Autumn	0.80	0.94	38.42
	Winter	0.67	0.51	67.53
100	Spring, Summer	0.64	0.64	121.37
	Autumn	0.70	1.19	52.11
	Winter	0.62	0.64	89.24

NHESSD
1, 1619–1649, 2013

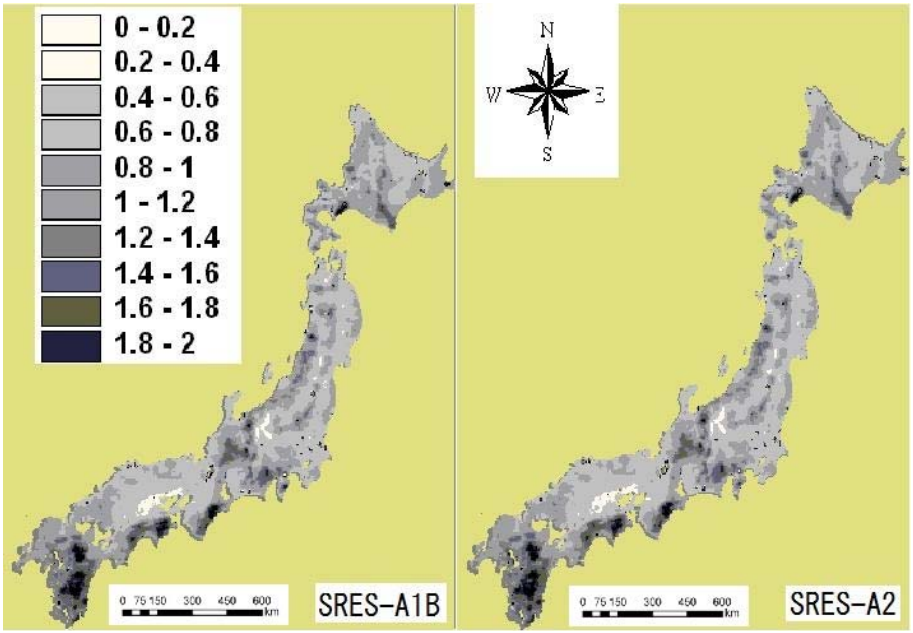

Fig. 1. Distribution of the fine-resolution factor (Bd).

NHESSD
1, 1619–1649, 2013

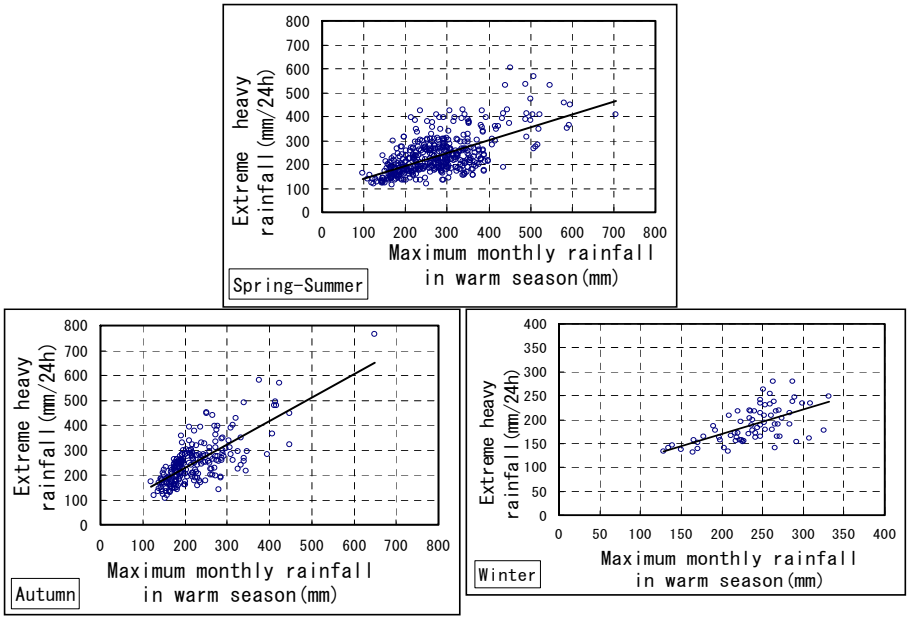

Fig. 2. Relationships between maximum monthly rainfall in each season and the extreme rainfall for a 30 yr return period.

NHESSD
1, 1619–1649, 2013

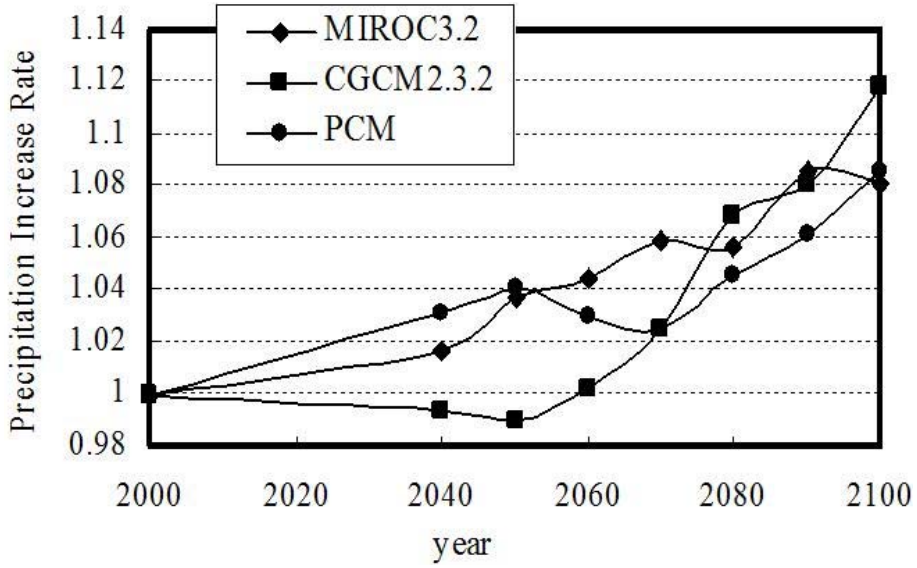

Fig. 3. Rates of precipitation increase predicted by MIROC, CGCM and PCM GCMs for the A1B SRESS scenario.

NHESSD
1, 1619–1649, 2013

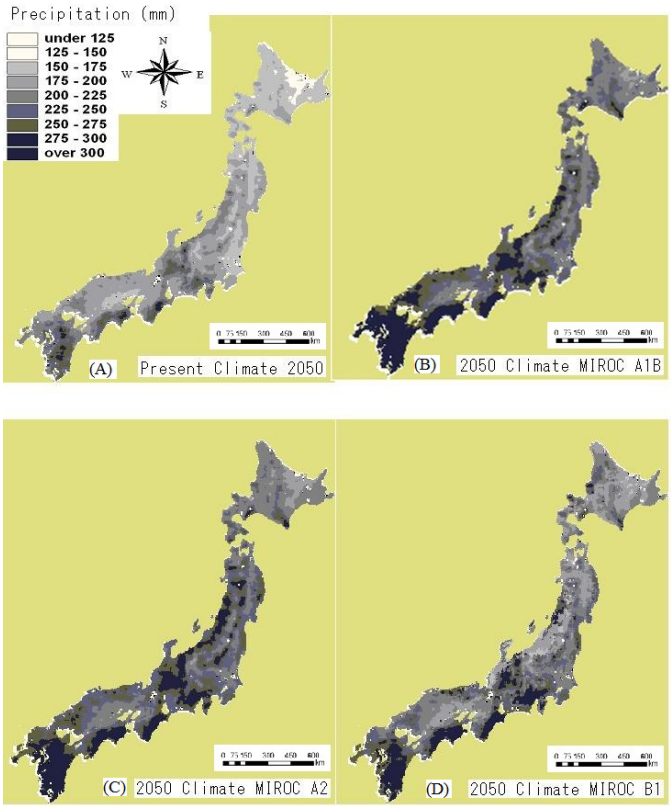

Fig. 4. Distribution of the daily extreme rainfall of **(A)** the present climate (in 2000), **(B)** MIROC's prediction for scenario A1B in 2050, **(C)** MIROC's prediction for scenario A2 in 2050 and **(D)** MIROC's prediction for B1 in 2050, all for a 50 yr return period.

NHESSD
1, 1619–1649, 2013

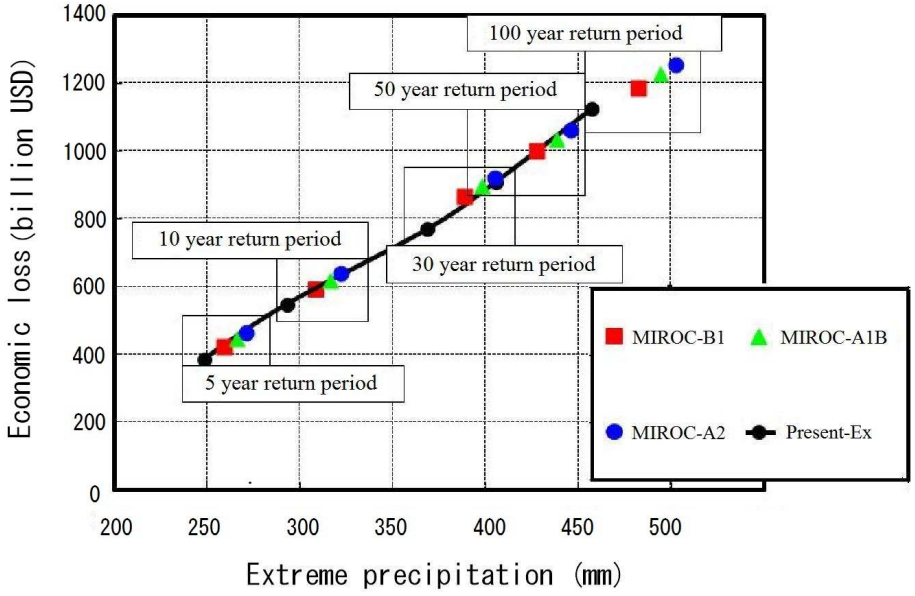

Fig. 5. Relationship between the variation in total economic loss due to flood damage in Japan and extreme rainfall.

NHESSD
1, 1619–1649, 2013

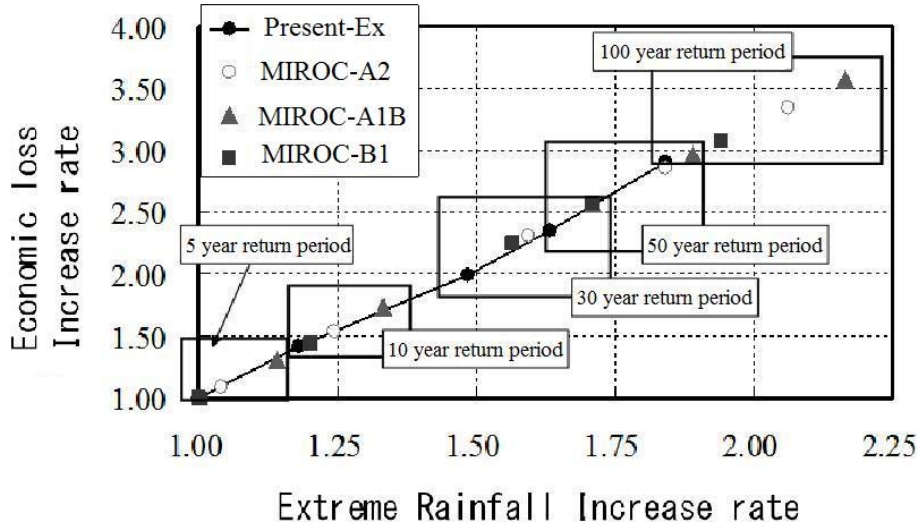

Fig. 6. Relationship between the increase in extreme rainfall and the increase in potential economic loss due to flood damage under the current climate.

NHESSD
1, 1619–1649, 2013

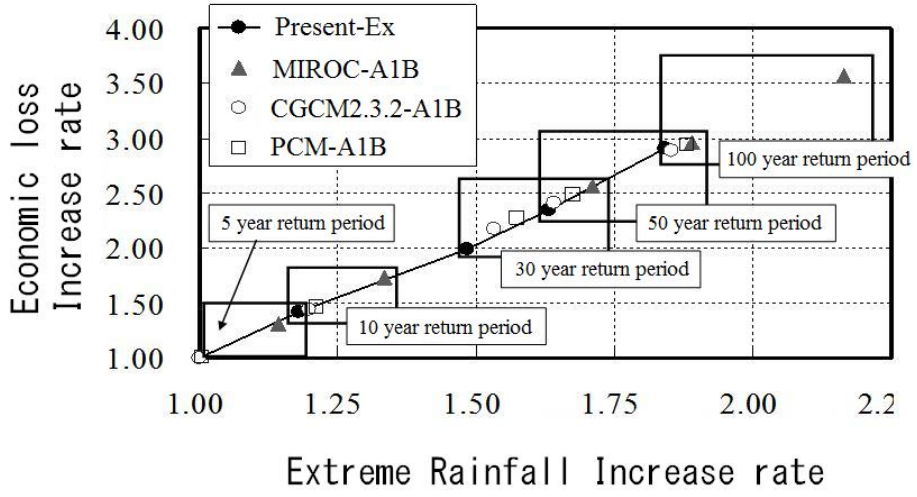

Fig. 7. Relationship between extreme rainfall and potential economic loss due to flood damage under the current climate and in 2050 as predicted by all GCMs.

NHESSD
1, 1619–1649, 2013